

F. J. Sciulli, Phys. Rev. Lett. **17**, 980 (1966).

<sup>86</sup>R. J. Abrams, A. Abashian, R. E. Mischke, B. M. K. Nefkens, J. H. Smith, R. C. Thatcher, L. J. Verhey, and A. Wattenberg, Phys. Rev. **176**, 1603 (1968).

<sup>87</sup>M. J. Longo, K. K. Young, and J. A. Helland, Phys. Rev. **181**, 1808 (1969).

<sup>88</sup>J. Smith (private communication).

## Study of the decay distributions of the $\eta'$ meson\*

C. Baltay, D. Cohen, S. Csorna, M. Habibi,<sup>†</sup> and M. Kalelkar  
Columbia University, New York, New York 10027

W. D. Smith and N. Yeh  
State University of New York at Binghamton, Binghamton, New York 13901  
(Received 5 March 1974)

We have carried out a study of the decay distributions of  $\eta'(958)$  mesons produced in the reaction  $K^-p \rightarrow \Lambda\eta'$  at 1.75 GeV/c, utilizing both the  $\eta\pi^+\pi^-$  and  $\pi^+\pi^-\gamma$  decay modes of the  $\eta'$ . A Dalitz-plot analysis of the  $\eta\pi^+\pi^-$  decay channel rules out all spin-parity assignments except  $0^-$  and  $2^-$ , but is unable to distinguish between them. We find no evidence for the existence of anisotropies in the  $\eta'$  decay angular distributions, and thus our data do not support the recent conjecture, based on the observation of such anisotropies, that the  $\eta'$  has spin 2.

### I. INTRODUCTION

The  $\eta'(958)$  meson was discovered about 10 years ago,<sup>1</sup> and many subsequent investigations have sought to determine its spin-parity assignment.<sup>2</sup> Dalitz-plot analyses of the  $\eta'$  decays have ruled out all assignments except  $J^{PC} = 0^{-+}$  and  $2^{-+}$ , with the  $0^{-+}$  assignment being favored. Since a spin-zero particle must decay isotropically in its center of mass, various attempts have been made to find evidence for a spin different from zero by searching for anisotropies in the  $\eta'$  decay distributions. Until recently, all such attempts proved fruitless, thus lending strong support to the  $0^-$  spin-parity assignment of the  $\eta'$ . A Brookhaven-Michigan collaboration,<sup>3</sup> however, has recently studied the decay angular distributions of  $\eta'$  mesons produced in the extreme forward direction in the reaction  $K^-p \rightarrow \Lambda\eta'$  at 2.18 GeV/c. They have found evidence that these forward-produced  $\eta'$  mesons have anisotropic decay distributions with respect to the incident beam, suggesting the possibility that the  $\eta'$  has  $J^P = 2^-$ . The confirmation of this spin-parity assignment would, of course, force us to revise the current SU(3) particle-classification scheme, which has the  $\eta'$  belonging to the pseudoscalar-meson nonet along with the  $\pi$ ,  $K$ , and  $\eta$  mesons.

We have carried out a study of the decay distributions of the  $\eta'$  meson utilizing the reaction  $K^-p \rightarrow \Lambda\eta'$  at an incident  $K^-$  momentum of 1.75 GeV/c. We have performed an analysis of the  $\eta'$  Dalitz plot and find the distribution of events to be

consistent with only the  $0^{-+}$  and  $2^{-+}$   $J^{PC}$  assignments for the  $\eta'$ . We have also searched for anisotropies in the decay angular distributions of forward-produced  $\eta'$  mesons. Unlike the Brookhaven-Michigan analysis, we do not find any evidence for the existence of such anisotropies, and thus our data do not lend additional support to the hypothesis of a spin-2  $\eta'$  suggested by their analysis.

### II. EXPERIMENTAL PROCEDURE

The data used in the present analysis are derived from an exposure of the Brookhaven National Laboratory 31-in. hydrogen bubble chamber to a beam of 1.75-GeV/c  $K^-$  mesons. The particular sample discussed here represents approximately 60% of the total exposure of 860 000 pictures and corresponds to  $\sim 23$  events/ $\mu\text{b}$ . All two-pronged events with an associated neutral decay were measured on the Columbia HPD (Hough-Powell device),<sup>4</sup> and subsequently passed through the reconstruction and kinematic fitting programs. It is from these events that we have obtained our data sample corresponding to the reaction

$$K^-p \rightarrow \Lambda\eta'. \quad (1)$$

Since only two-pronged events with associated neutral decays have been analyzed, we will be discussing only the following two subsets of reaction (1):

$$\begin{aligned} K^-p &\rightarrow \Lambda\eta', \\ \eta' &\rightarrow \pi^+\pi^-\eta_N, \\ \eta_N &\rightarrow \text{neutrals} \end{aligned} \quad (2)$$

and

$$\begin{aligned} K^- p &\rightarrow \Lambda \eta', \\ \eta' &\rightarrow \pi^+ \pi^- \gamma. \end{aligned} \quad (3)$$

#### A. Selection of the $\eta' \rightarrow \pi^+ \pi^- \eta$ sample

In order for an event to be considered as a candidate for either reaction (2) or (3), the associated neutral decay was required to make an acceptable three-constraint fit to a  $\Lambda$  produced at the event vertex. We denote by  $M^2$  the square of the missing mass recoiling from the  $\Lambda$  and the two charged particles for all such events when the charged particles are interpreted as pions, and display in Fig. 1(a) the distribution in  $M^2$  for values of  $M^2 \geq 0.15 \text{ GeV}^2$ . A sharp peak is clearly discernible at the square of the  $\eta$  mass. We proceeded to fit all such events with values of  $M^2 \geq 0.15 \text{ GeV}^2$  to the four-constraint hypothesis

$$K^- p \rightarrow \Lambda \pi^+ \pi^- \eta. \quad (4)$$

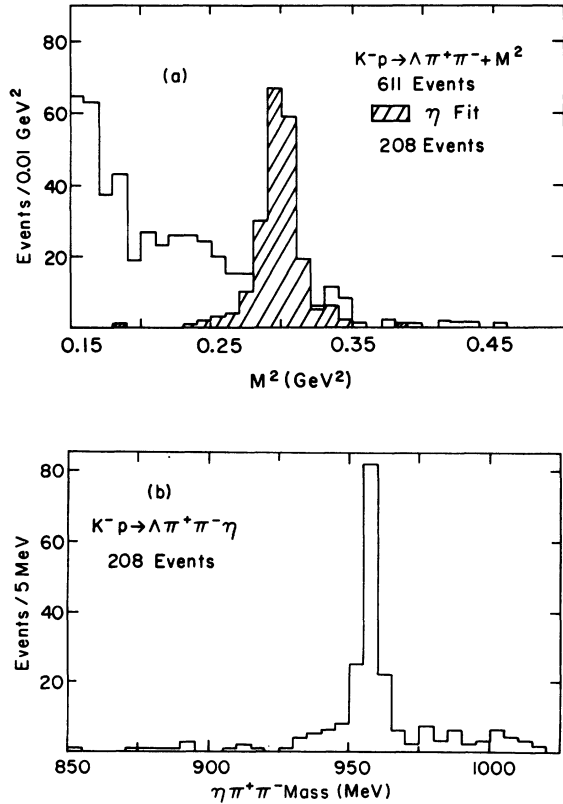


FIG. 1. (a) The square of the missing mass recoiling from the  $\Lambda \pi^+ \pi^-$  system for two-pronged events with an associated  $\Lambda$ , shown for values  $\geq 0.15 \text{ GeV}^2$ . The shaded region shows those events that made acceptable fits to the missing- $\eta$  hypothesis. (b) The  $\eta \pi^+ \pi^-$  mass spectrum for the reaction  $K^- p \rightarrow \Lambda \pi^+ \pi^- \eta$ .

A total of 208 events made acceptable fits to this hypothesis, and these events are displayed as the shaded region of Fig. 1(a). We show in Fig. 1(b) the  $\eta \pi^+ \pi^-$  mass spectrum for those events successfully fitting reaction (4). This distribution shows a clear  $\eta'$  signal at  $\sim 960 \text{ MeV}$  with very little background beneath it. Our final  $\eta'$  data sample corresponding to reaction (2) was obtained by accepting those events fitting reaction (4) whose  $\eta \pi^+ \pi^-$  mass lies between 950 and 970 MeV. This cut resulted in a final sample of 134 events. In order to normalize all accepted events to an  $\eta'$  mass of 958 MeV, these events were further fitted to the five-constraint hypothesis of reaction (2), and it is these fitted parameters which were used in the ensuing analysis.

A source of background in our final sample for reaction (2) arises from the fact that events belonging to the reaction

$$\begin{aligned} K^- p &\rightarrow \Lambda \eta', \\ \eta' &\rightarrow \pi^0 \pi^0 \eta_c, \\ \eta_c &\rightarrow \pi^+ \pi^- \pi^0 (\gamma) \end{aligned} \quad (5)$$

are indistinguishable from events belonging to reaction (2) when the invariant mass of the two  $\pi^0$ 's from the  $\eta' \rightarrow \pi^0 \pi^0 \eta_c$  decay and the neutral particle from the subsequent decay of the  $\eta_c$  overlaps the  $\eta$  mass region. In order to ascertain the magnitude of the background present due to events belonging to reaction (5), we have used a Monte Carlo program to generate, for each event identified as belonging to reaction (2), several  $\eta$  decays into  $\pi^+ \pi^- \pi^0$  and  $\pi^+ \pi^- \gamma$  using the measured matrix elements and relative magnitudes for these decays.<sup>5</sup> We have examined the invariant mass spectrum of the  $\pi^+ \pi^-$  from the  $\eta' \rightarrow \pi^+ \pi^- \eta$  decay combined with the  $\pi^0$  or  $\gamma$  from the  $\eta \rightarrow \pi^+ \pi^- \pi^0 (\gamma)$  decay. From the degree of overlap this mass spectrum has with the  $\eta$  mass region, and from isotopic-spin considerations and the measured  $\eta$  branching ratios, we have determined the background due to reaction (5) to be  $(7 \pm 1)\%$ . The  $\eta$  mass region was taken to be 530 to 570 MeV since this was essentially the  $\eta$  mass region selected by the fit to reaction (4). Not only does the technique described above provide us with a measurement of the background present in our event sample for reaction (2), but it also provides us with the decay distributions for these background events. These have been examined and will be discussed later.

#### B. Selection of the $\eta' \rightarrow \pi^+ \pi^- \gamma$ sample

The separation of the reaction

$$K^- p \rightarrow \Lambda \pi^+ \pi^- \gamma \quad (6)$$

from the reactions

$$K^-p \rightarrow \Lambda \pi^+ \pi^-, \quad (7)$$

$$K^-p \rightarrow \Sigma^0 \pi^+ \pi^-, \quad (8)$$

and

$$K^-p \rightarrow \Lambda \pi^+ \pi^- \pi^0 \quad (9)$$

is extremely difficult owing to the proximity of the missing mass for these four reactions. We have not considered as candidates for reaction (6) any events making successful fits to the highly constrained reactions (7) or (8). This cut excludes some of the events belonging to reaction (6) (e.g., some events with low-momentum  $\gamma$ 's), and we discuss later its possible effect on our analysis. Of the remaining events making successful fits to reaction (6), most also fit the hypothesis of reaction (9). Fit ambiguities between these two reactions were partially resolved by examining the probability for  $M^2$ , the square of the missing mass recoiling from the  $\Lambda \pi^+ \pi^-$  system, being consistent with either a  $\gamma$  or a  $\pi^0$ . In Fig. 2, we show the  $M^2$  distribution after removing events making successful fits to either reaction (7) or (8). Two peaks are clearly discernible, one due to events with a missing  $\gamma$ , and the other due to events with a missing  $\pi^0$ . For cases when the probability difference between the two choices was not large enough to resolve the ambiguity ( $\sim 50\%$  of the time), we accepted as belonging to reaction (6) those events having values of  $M^2 < 0.003 \text{ GeV}^2$ . Although this cut excludes some genuine  $\Lambda \pi^+ \pi^- \gamma$  events from our sample, this exclusion is accomplished in an

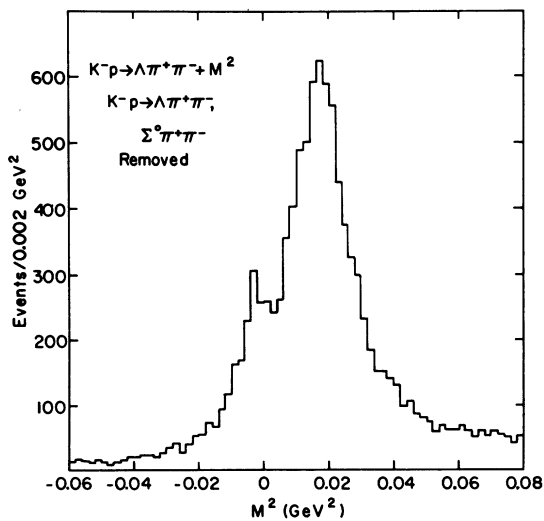


FIG. 2. The square of the missing mass recoiling from the  $\Lambda \pi^+ \pi^-$  system for two-pronged events with an associated  $\Lambda$ . Events making acceptable fits to the reactions  $K^-p \rightarrow \Lambda \pi^+ \pi^-$  and  $K^-p \rightarrow \Sigma^0 \pi^+ \pi^-$  have been removed.

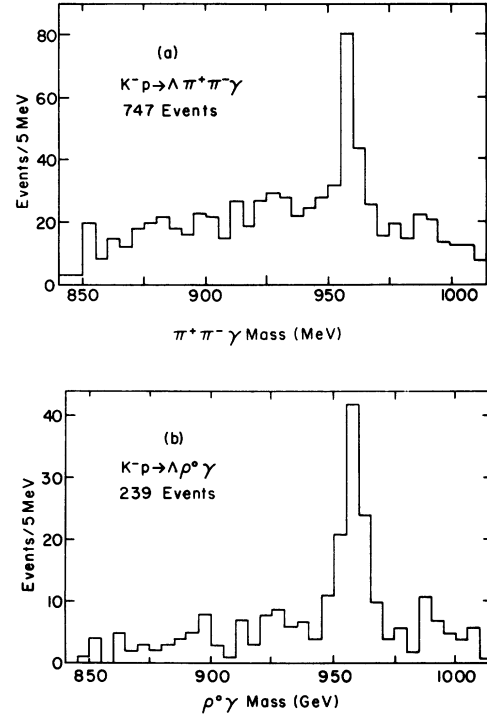
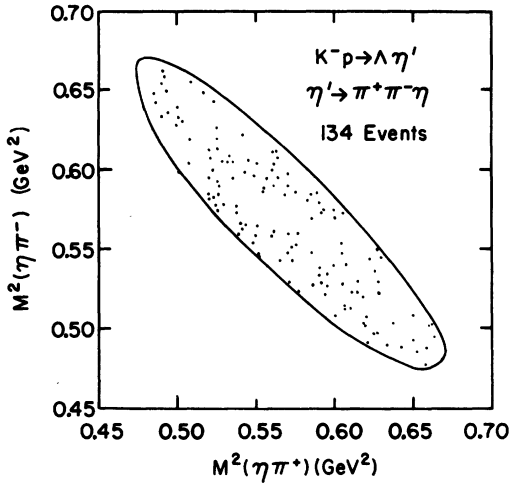


FIG. 3. (a) The  $\pi^+ \pi^- \gamma$  mass spectrum for the reaction  $K^-p \rightarrow \Lambda \pi^+ \pi^- \gamma$ . (b) The  $\rho^0 \gamma$  mass spectrum for the reaction  $K^-p \rightarrow \Lambda \rho^0 \gamma$ . The  $\rho$  mass region was chosen to span 640 to 900 MeV.

essentially bias-free manner. Moreover, this cut is extremely effective in eliminating a large fraction of the  $\Lambda \pi^+ \pi^- \pi^0$  background (see Fig. 2). We note that since we are interested in studying the  $\eta'$  meson, the above selection criteria were only applied to events having a missing mass recoiling from the  $\Lambda$  greater than 850 MeV.

After imposing the above criteria, a total of 747 events having a missing mass recoiling from the  $\Lambda$  greater than 850 MeV were accepted as belonging to reaction (6). The  $\pi^+ \pi^- \gamma$  mass spectrum for these events is shown in Fig. 3(a). Again, the  $\eta'$  is prominent at a mass value of  $\sim 960$  MeV. We display in Fig. 3(b) the  $\rho^0 \gamma$  invariant-mass distribution for these same events, where we have chosen the  $\rho$  mass region to span 640 to 900 MeV. A comparison of Figs. 3(a) and 3(b) indicates that our data are consistent with virtually all the  $\eta' \rightarrow \pi^+ \pi^- \gamma$  decays being in reality  $\eta' \rightarrow \rho^0 \gamma$  decays. Thus, our final data sample for reaction (3) was obtained by imposing the additional cut on the above sample that the  $\rho^0 \gamma$  mass lie between 950 and 970 MeV. This resulted in a final sample consisting of 97 events. As before, these events were further fitted to the five-constraint hypothesis of reaction (3), and it is these fitted parameters which were used in the ensuing analysis.

FIG. 4. The  $\eta'$  Dalitz plot for the  $\pi^+\pi^-\eta$  decay mode.

### III. ANALYSIS

We display in Fig. 4 the  $\eta'$  Dalitz plot for the  $\pi^+\pi^-\eta$  decay mode [reaction (2)]. We have fitted this Dalitz plot to the predictions of various quantum-number assignments for  $\eta'$  spin values of 0, 1, and 2. The forms of the squared matrix elements, summed over the spin states of the  $\eta'$ , for the various quantum-number assignments that were fitted are listed in Table I.<sup>8</sup> These correspond to the simplest matrix elements which can be constructed for the various  $\eta'$  quantum numbers. The results of our fits are also shown in Table I, and indicate that the  $0^{-+}$  assignment is strongly favored over all other simple  $J^{PC}$  matrix elements. However, a mixture of the two simplest  $2^{-+}$  amplitudes also provides a good descrip-

tion of the Dalitz-plot distribution; the best-fit mixture is indicated in this table. We thus reach the same conclusions as have all such previous studies,<sup>7</sup> namely, that the Dalitz-plot analysis is not able to distinguish between the  $0^-$  and  $2^-$  spin-parity assignments of the  $\eta'$ . It is also possible that by using more complicated matrix elements, other spin-parity assignments could describe the data as well as the  $0^-$  and  $2^-$  assignments. We have also examined the Dalitz-plot distribution expected from the  $\sim 7\%$  background events present due to reaction (5) using the generated events as discussed in Sec. II. These background events do not introduce any appreciable distortion of the  $\eta'$  Dalitz plot.

We have also carried out a study of the decay angular distributions of the  $\eta'$ . For the  $\pi^+\pi^-\eta$  decay mode, we have examined the angular distribution of the line of flight of the  $\eta$  ( $\hat{n}$ ) and the normal to the  $\eta'$  decay plane ( $\hat{n}'$ ), both calculated in the  $\eta'$  rest frame. For the  $\rho^0\gamma$  decay mode, we have investigated the distribution of the  $\gamma$  direction ( $\hat{\gamma}$ ) in the  $\eta'$  rest frame. All distributions are calculated in the coordinate system whose  $z$  axis is chosen to be the beam direction in the  $\eta'$  rest frame, while the production plane normal is chosen as the  $y$  axis, and the  $x$  axis is chosen so as to make the coordinate system right-handed. Both the polar ( $\cos\theta$ ) and azimuthal ( $\phi$ ) angular distributions for all three analyzing vectors are shown in Fig. 5.

For  $J^P = 0^-$   $\eta'$  mesons, the decay angular distributions must be isotropic. For  $J^P = 2^-$   $\eta'$  mesons, it is conceivable that the production mechanism could produce isotropic decay angular distributions, but for particles with nonzero spin,

TABLE I. Results of the Dalitz-plot analysis of the  $\eta' \rightarrow \eta\pi^+\pi^-$  decay.<sup>a</sup>

$J^{PC}$	$l_\eta$	$l_{\pi\pi}$	$ M ^2$	Probability
$0^{-+}$	0	0	1	0.79
$1^{++}$	1	0	$k^2$	$<10^{-4}$
$1^{-+}$	2	2	$q^4 k^4 \cos^2\theta \sin^2\theta$	$<10^{-4}$
$2^{++}$	1	2	$q^4 k^2 \sin^2\theta$	$<10^{-4}$
$2^{-+}$	0	2	$q^4$	$<10^{-4}$
$2^{-+}$	2	0	$k^4$	$<10^{-4}$
$2^{-+}$			$q^4 + \text{Re}(a)q^2 k^2(3\cos^2\theta - 1) +  a ^2 k^4$	0.83 <sup>b</sup>
$0^{--}$	1	1	$q^2 k^2 \cos^2\theta$	$<10^{-4}$
$1^{+-}$	0	1	$q^2$	0.009
$1^{--}$	1	1	$q^2 k^2 \sin^2\theta$	0.003
$2^{+-}$	2	1	$q^2 k^4 \sin^2\theta$	$<10^{-4}$
$2^{--}$	1	1	$q^2 k^2(3 + \cos^2\theta)$	0.028

<sup>a</sup> $l_\eta$  is the orbital angular momentum of the  $\eta$  in the  $\eta'$  rest frame,  $l_{\pi\pi}$  is that of the two pions in the  $\pi\pi$  rest frame,  $q$  is the momentum of the pion in the  $\pi\pi$  rest frame,  $k$  is the momentum of the  $\eta$  in the  $\eta'$  rest frame, and  $\theta$  is the angle between the  $\pi^+$  and the  $\eta$  in the  $\pi\pi$  rest frame.  $|M|^2$  is summed over spins.

<sup>b</sup>The best-fit values are  $\text{Re}(a) = 0 \pm 0.12$ ,  $\text{Im}(a) = 0.36 \pm 0.08$ .

this is generally not the case. None of the distributions presented in Fig. 5 show any evidence for anisotropies. We note that for the  $\eta' \rightarrow \rho^0 \gamma$  decay, we have also examined the background-subtracted decay distributions, and these also fail to show any evidence for anisotropies. We have, in addition, performed a moment analysis on all of the above decay distributions, and observe no pattern of statistically significant nonzero moments. Thus, these decay distributions give no evidence to support the hypothesis of a spin-2  $\eta'$ .

Adair,<sup>8</sup> however, has pointed out the utility of confining a study of the decay distributions of a particle whose spin is unknown to particles produced in the extreme forward direction. The motivation for this procedure is that for particles produced in the forward direction, the projection of the final-state orbital angular momentum along

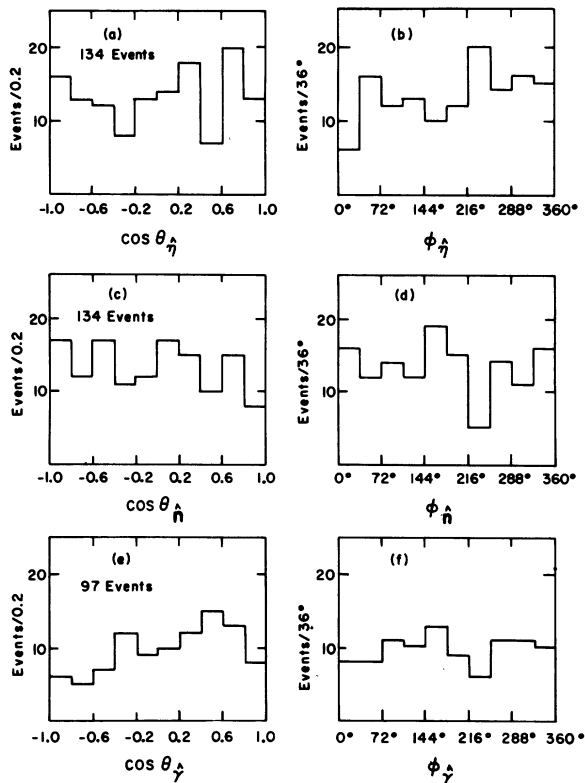


FIG. 5. Polar ( $\cos\theta$ ) and azimuthal ( $\phi$ ) angular distributions for the  $\eta'$  decay vectors discussed in the text. All distributions are calculated in the coordinate system whose  $z$  axis is chosen to be the beam direction in the  $\eta'$  rest frame, while the production plane normal is chosen as the  $y$  axis, and the  $x$  axis is chosen so as to make the coordinate system right-handed. (a) and (b) refer to the direction of the  $\eta'$  in the  $\eta'$  rest frame for the  $\pi^+\pi^-\eta$  decay mode, (c) and (d) refer to the normal to the  $\eta'$  rest frame for the  $\pi^+\pi^-\eta$  decay mode, and (e) and (f) refer to the  $\gamma$  direction in the  $\eta'$  rest frame for the  $\rho^0\gamma$  decay mode.

the beam direction ( $L_z$ ) must be zero. This limits the spin-projection states that can be populated by the particle under consideration, and thus limits the form of this particle's decay angular distribution. In particular, if the  $\eta'$  were a spin-2 particle, it could, in general, populate all five spin-projection states (0,  $\pm 1$ , and  $\pm 2$ ). However, if we restrict ourselves to  $\eta'$  mesons produced in the forward direction in the reaction  $K^-p \rightarrow \Lambda\eta'$ , then, as stated above, the projection of the final-state orbital angular momentum along the beam direction must be zero, and only the three  $\eta'$  states with spin projections of 0 and  $\pm 1$  are allowed. Thus, even if the  $\eta'$  were a spin-2 particle and its over-all decay angular distributions were isotropic, the elimination of the states with spin projections of  $\pm 2$  should introduce anisotropies into these distributions. The decay angular distributions for a spin-zero  $\eta'$  must, of course, be isotropic whether the sample considered is restricted to forward-produced  $\eta'$  mesons or not. The exact forms of the distributions expected for  $\eta'$  mesons produced in the forward direction depends on the relative amplitudes of the states with spin-projection magnitudes of 0 and 1. These distributions have been calculated for both the  $\pi^+\pi^-\eta$  and  $\rho^0\gamma$  decay modes of the  $\eta'$ .<sup>9</sup>

A Brookhaven-Michigan collaboration<sup>3</sup> has studied the decay angular distributions of  $\eta'$  mesons produced in the extreme forward direction in reaction (1) at 2.18 GeV/c, and have found some evidence that the forward-produced  $\eta'$  mesons do have anisotropic decay distributions with respect to the incident beam. We have also examined the decay angular distributions for forward-produced  $\eta'$  mesons. In order to select the event sample for which the projection of the final-state orbital angular momentum along the beam is minimal,<sup>10</sup> we have examined the  $\cos\theta_{c.m.}$  distribution for all events belonging to either the  $\pi^+\pi^-\eta$  or  $\pi^+\pi^-\gamma$  decay modes [reaction (2) or (3)], where we define  $\theta_{c.m.}$  to be the angle of the  $\eta'$  with respect to the incident  $K^-$  in the over-all  $K^-p$  center-of-mass system. This distribution is shown in Fig. 6. The solid curve drawn on this figure is the result of a fit to this distribution to a power series in  $\cos\theta_{c.m.}$ . Only terms up to second order in  $\cos\theta_{c.m.}$  are used since the inclusion of higher-order terms did not improve the quality of the fit. The fact that only terms up to  $\cos^2\theta_{c.m.}$  are needed to obtain a good fit to this distribution indicates that the highest orbital angular momentum wave present in the  $\Lambda\eta'$  final state is  $L=1$ . The fact that higher orbital angular momentum waves are not present is not surprising since we are only 56 MeV above  $\Lambda\eta'$  threshold in this experiment. Written in a way that explicitly displays the con-

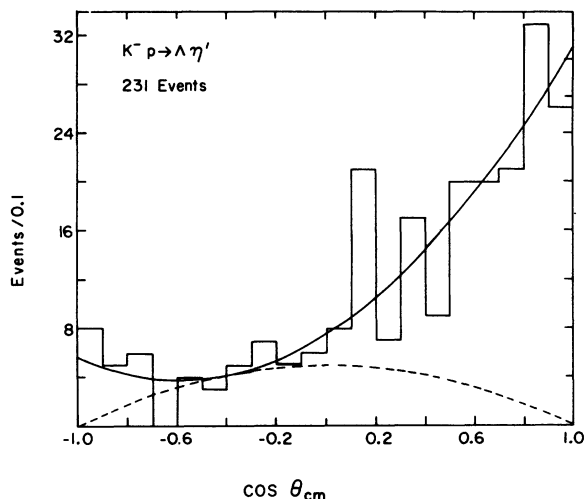


FIG. 6.  $\cos\theta_{c.m.}$  distribution for the reaction  $K^-p \rightarrow \Lambda\eta'$  for both the  $\pi^+\pi^-\eta'$  and  $\pi^+\pi^-\gamma$  decay modes, where  $\theta_{c.m.}$  is the angle of the  $\eta'$  with respect to the incident  $K^-$  in the  $K^-p$  center-of-mass system. The solid curve is the result of a fit of this distribution to the form  $a + b \cos\theta_{c.m.} + c \cos^2\theta_{c.m.}$ , while the dashed curve shows the maximum possible contribution of the  $L_x = \pm 1$  terms (see text).

tribution of the different spin-projection amplitudes, the angular distribution of an  $L = 1$  state is

$$f(\theta_{c.m.}) = |A + B \cos\theta_{c.m.}|^2 + |C|^2 \sin^2\theta_{c.m.},$$

where the first term represents the contribution of the  $L_x = 0$  amplitude and the second the contribution of the  $L_x = \pm 1$  amplitudes. ( $\hat{z}$  is here the direction of the incident  $K^-$  in the over-all center-of-mass system.) Although  $A$ ,  $B$ , and  $C$  cannot be uniquely determined from our angular distribution, the maximum possible contribution of the  $L_x = \pm 1$  terms ( $|C|^2 \sin^2\theta_{c.m.}$ ) is represented as the dashed curve in Fig. 6. It is thus clear from this figure that in order to have a negligible contribution from the  $L_x = \pm 1$  terms, it is sufficient to restrict our analysis to  $\eta'$  mesons produced with  $\cos\theta_{c.m.} > 0.6$ .

Making the above  $\cos\theta_{c.m.}$  cut leaves us with 58  $\eta' \rightarrow \eta\pi^+\pi^-$  events and 42  $\eta' \rightarrow \rho^0\gamma$  events. We show in Fig. 7 the decay angular distributions for this restricted event sample. No anisotropies are evident in our data even after restricting ourselves to  $\eta'$  mesons produced in the forward direction. This result is in contrast to the conclusions reached in Ref. 3. We summarize these results in Table II by presenting the number of polar events ( $|\cos\theta| > 0.5$ ) and the number of equatorial events ( $|\cos\theta| < 0.5$ ) for each of the distributions studied, and also present results from Ref. 3 for

purposes of comparison. We note that an isotropic distribution (spin 0) is characterized by an equal number of polar and equatorial events, while a spin-2  $\eta'$  would result in more polar than equatorial events for the  $\hat{n}$  distribution, and fewer polar than equatorial events for the  $\hat{n}$  and  $\hat{\gamma}$  distributions.<sup>3,9</sup> The magnitude of these differences for a spin-2  $\eta'$  would depend on the relative amplitudes of the states with spin-projection magnitudes of 0 and 1. Our numbers do not show any statistically significant deviation from isotropy, and thus, while we cannot rule out the spin-2 assignment for the  $\eta'$ , our data certainly provide no evidence for it. We have also examined the background-subtracted distributions for the  $\eta' \rightarrow \rho^0\gamma$  decay mode, and the numbers obtained in this case are virtually identical to those listed in Table II. In addition, we have studied the decay distributions using as  $z$  axis the direction of the incident beam in the over-all center-of-mass system instead of the direction of the beam in the  $\eta'$  rest frame. The numbers presented in Table II remain essentially unchanged. Thus, with statistics comparable to those of the Brookhaven-Michigan collaboration,

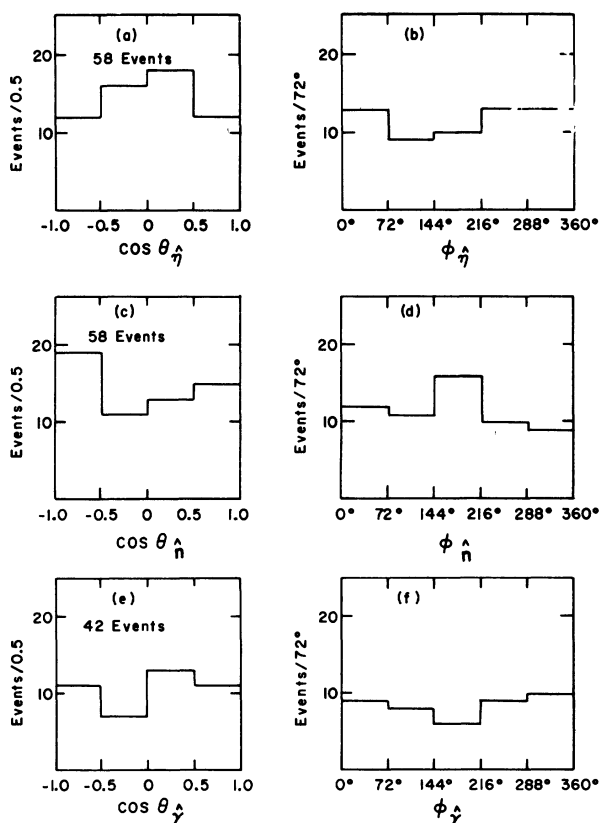


FIG. 7. Polar ( $\cos\theta$ ) and azimuthal ( $\phi$ ) angular distributions for the  $\eta'$  decay vectors for  $\eta'$  mesons produced with  $\cos\theta_{c.m.} > 0.6$ .

TABLE II. Number of polar events ( $P$ ) and number of equatorial events ( $E$ ) for each of the three  $\eta'$  decay angular distributions discussed in the text. Results are presented for this experiment and for the Brookhaven-Michigan experiment (Ref. 3).  $N\sigma$  refers to the number of standard deviations the respective entries differ from equal numbers of  $P$  and  $E$  (an isotropic distribution).

Vector	This experiment			Brookhaven-Michigan		
	$P$	$E$	$N\sigma$	$P$	$E$	$N\sigma$
$\hat{\eta}$	24	34	1.3	39	27	1.5
$\hat{\eta}$	34	24	1.3	23	43	2.5
$\hat{\rho}$	22	20	0.3	7	20	1.5 <sup>a</sup>

<sup>a</sup>These are background-subtracted numbers.

we fail to observe any anisotropies in the decay angular distributions of forward-produced  $\eta'$  mesons. We note that we have also repeated the above analysis restricting ourselves to  $\eta'$  mesons produced with  $\cos\theta_{c.m.} > 0.8$ , and our conclusions remain unchanged.

We have carried out several checks to ensure that any anisotropies that might be present were not masked by experimental biases. In particular, we have examined the decay angular distributions of the  $\sim 7\%$  background events present in the data sample for the  $\pi^+\pi^-\eta$  decays [reaction (2)] due to events belonging to reaction (5). These distributions were not found to exhibit any significant anisotropies. For the  $\pi^+\pi^-\gamma$  decay mode, the removal of events making successful fits to either reaction (7) or (8) from the data sample for reac-

tion (6) introduces a possible bias against  $\gamma$ 's emitted in the backward direction in the center-of-mass system, and consequently a possible bias against backward  $\gamma$ 's in our distributions. A slight loss of events due to this cut might have occurred near  $\cos\theta = -1$  in the over-all distribution of Fig. 5(e); however, when confining ourselves to forward-produced  $\eta'$  mesons [Fig. 7(e)], there is no evidence for any significant loss. We have also carried out a study of possible biases introduced due to uncertainties in the beam momentum or its error used in the kinematic fitting program SQUAW, and found that neither of these effects could have caused any significant changes in the numbers displayed in Table II.

#### IV. CONCLUSIONS

We have carried out a study of the decay distributions of the  $\eta'$  meson utilizing the  $\eta' \rightarrow \eta\pi^+\pi^-$  and  $\eta' \rightarrow \pi^+\pi^-\gamma$  decay modes. A Dalitz-plot analysis of the  $\eta\pi^+\pi^-$  decay of the  $\eta'$  has ruled out all spin-parity assignments except  $0^-$  and  $2^-$ , but is unable to distinguish between these two possibilities. We have searched for anisotropies in the decay angular distributions of the  $\eta'$  and have found no evidence for the existence of any. Even upon confining our analysis to  $\eta'$  mesons produced in the forward direction, we were unable to detect any anisotropies. We thus conclude that, while we are unable to rule out the spin-2 assignment for the  $\eta'$ , our data do not support this hypothesis, in contrast to a similar analysis<sup>3</sup> carried out recently which claims evidence for a spin-2  $\eta'$ .

\*Research supported by the National Science Foundation and the U. S. Atomic Energy Commission.

†Present address: Brookhaven National Laboratory, Upton, New York.

<sup>1</sup>G. Kalbfleisch *et al.*, Phys. Rev. Lett. **12**, 527 (1964); M. Goldberg *et al.*, *ibid.* **12**, 546 (1964).

<sup>2</sup>For a complete list of references, see Particle Data Group, Rev. Mod. Phys. **45**, S1 (1973).

<sup>3</sup>G. Kalbfleisch *et al.*, Phys. Rev. Lett. **31**, 333 (1973); J. Danburg *et al.*, Phys. Rev. D **8**, 3744 (1973).

<sup>4</sup>For a complete discussion of the scanning and measuring procedure, see M. Habibi, Ph.D. thesis, Columbia University, Nevis Report No. 199, 1973 (unpublished). See also, C. Baltay *et al.*, Phys. Rev. D **9**, 49 (1974) and C. Baltay *et al.*, in *Baryon Resonances—73*, pro-

ceedings of the Purdue Conference on Baryon Resonances, 1973, edited by E. C. Fowler (Purdue Univ. Press, Lafayette, Indiana, 1973), p. 387.

<sup>5</sup>J. Layter *et al.*, Phys. Rev. D **7**, 2565 (1973); C. Baltay, in *Meson Spectroscopy*, edited by C. Baltay and A. H. Rosenfeld (Benjamin, New York, 1968), p. 95; see also Ref. 2.

<sup>6</sup>A. Rittenberg, Ph.D. thesis, Lawrence Radiation Laboratory Report No. UCRL-18863, 1969 (unpublished).

<sup>7</sup>See, for example, M. Aguilar-Benitez *et al.*, Phys. Rev. D **6**, 29 (1972). See also Refs. 2, 3, and 6.

<sup>8</sup>R. Adair, Phys. Rev. **100**, 1540 (1955).

<sup>9</sup>V. Ogievetsky *et al.*, Phys. Lett. **35B**, 69 (1971); J. Klosinski *et al.*, Acta Phys. Polon. **B1**, 359 (1970).

<sup>10</sup>F. Eisler *et al.*, Nuovo Cimento **7**, 222 (1958).